Electronic spin-flipping collisions of hydrogen atoms

B. Zygelman*

Department of Physics and Astronomy, University of Nevada, Las Vegas, Las Vegas, Nevada 89154, USA

(Received 9 July 2009; published 8 March 2010)

We present a unified multichannel approach to calculate electron spin-exchange and spin-flipping transition cross sections for collisions of H with H, H with T, and T with T. We use the theory to calculate the hyperfine quenching cross sections for collision energies that range from 1 mK to thermal temperatures. We show that spin-flipping transitions are induced by the splitting of the $b\,^3\Sigma_u$ Born-Oppenheimer potential via the long-range magnetic interactions among electrons. We find that the spin-flipping cross sections in the tritium dimer are about a magnitude larger than that predicted by mass scaling the H-H cross sections. For the former, we show that the spin-exchange cross sections are several magnitudes larger, at cold temperatures, than that of the hydrogen system. We compare the results of the multichannel approach with those obtained using approximate methods such as the degenerate internal-state, the elastic, and Born approximations and discuss their respective range of validity.

DOI: 10.1103/PhysRevA.81.032506 PACS number(s): 34.50.Cx

I. INTRODUCTION

The 21 cm line of atomic hydrogen, corresponding to the ground state $F = 1 \rightarrow F = 0$ hyperfine transition has played an important role in radio astronomy [1]. Purcell [1] first noted the significance of atomic collisions in determining the spin temperature of hydrogen, a parameter used by astronomers to characterize H I regions. The advent of "21 cm cosmology" [2] focused renewed attention to understanding the processes that determine the hyperfine level populations of ground-state atomic hydrogen. Recent studies [3] demonstrated that favorable conditions of hydrogen gas temperature and density in the early universe, for $30 < z < 200$, may allow tomographic maps of this epoch. Spin-exchange [4–6] collisions play a crucial role in enabling that scenario [7]. This process describes collisions in which the total azimuthal spin angular momentum of the atom pair is conserved and which, since the electron and nuclear spins are coupled by the hyperfine interaction, induce hyperfine transitions. Spin exchange is precipitated by interference of the dynamic phase histories generated when the atoms approach in either their electronic singlet or triplet configurations [4–6]. Because the electronic energy splittings between the singlet and triplet states are on the order of chemical energies, spin-exchange cross sections are typically much larger than those of transitions induced by magnetic interactions among the atoms. In this article we denote the latter as spin-flipping transitions since, in that case, the change of total azimuthal spin angular momentum M is nonzero. Though spin-flipping cross sections are small, they are important if the hydrogen gas is polarized since selection rules for spin exchange do not allow relaxation of two hydrogen atoms in the same $F = 1, m \neq 0$ magnetic sublevel [7]. A major effort of this article is to present collision data including $\Delta M \neq 0$ spin-flipping cross sections for H-H collisions over a wide temperature range. Such data are important in accurate kinetic modeling of hydrogen gas in the early universe [8] and the hydrogen maser [9].

Substantial spin-exchange collision data exist, including the results of calculations [2,6,7,10,11] and measurements [12,13], however, there is a paucity of data for $\Delta M \neq 0$ spin-flipping processes. Calculations for magnetic level-changing transitions for hydrogen atoms in a magnetic field and at cryogenic temperatures were reported [14], but here we present data for collision energies within the mK to thermal energy range. Because the tritium atom has a similar hyperfine structure to hydrogen (tritium has a 1517 MHz hyperfine splitting compared to 1420 MHz for hydrogen [15]) we explore the substitution of H with T in our calculations. Advances in cooling atoms using Stark decelerators [16,17] may allow measurements for the cold collision properties of species, such as hydrogen and its isotopes, that were not as accessible in laboratory efforts that utilize laser and evaporative cooling technologies. Here, we present new results for H-T and T-T collision cross sections. Because magnetic interactions are weak, Born approximation methods were successful in predicting $\Delta M \neq 0$ cross sections at cold temperatures [18]. We compare our multichannel results with those predicted by the Born approximation and affirm that, for the H-H and H-T systems, the latter provides an excellent approximation at kinetic temperatures $\ll 1$ K. For the T-T system at cold temperatures, the Born approximation underestimates, even at temperatures $\approx$mK, the multichannel predictions by an order of magnitude. In all cases we find that the Born approximation fails at temperatures $T > \approx 1$ K.

Traditional close coupling methods typically include magnetic interactions as a perturbation to the standard Born-Oppenheimer (BO) description, which includes only electrostatic interactions of the collision. It has long been realized [4,6] that, in the alkali metals, spin exchange is driven by the energy splittings of the asymptotically degenerate $X\,^1\Sigma_g^+$ and $b\,^3\Sigma_u^+$ BO states in the molecular region. Here we introduce a collision formalism in which the magnetic interaction is included in our BO description. We diagonalize the total electronic Hamiltonian within the adiabatic approximation and find that the magnetic interactions split the $b\,^3\Sigma_u^+$ energy into two components. We show how this splitting results in nonvanishing $\Delta M \neq 0$ transition cross sections. In this

*bernard@physics.unlv.edu

way we make a connection to previous work involving fine-structure changing transitions [19], where it was shown how splittings of BO energies control the efficiency of the latter. Similar considerations were also discussed [20] in m-changing transitions induced by isotropic perturbers.

In Sec. II we present a theoretical overview of our close coupling theory. To simplify the discussion we work in the degenerate internal state (DIS) [9], or elastic [6], approximation. In that approximation the hyperfine structure splittings among the $F = 0$ and $F = 1$ hyperfine levels are ignored. Results from these calculations show that this approximation is very accurate for collision energies >1 K. It has the advantage of greatly simplifying the set of multichannel equations and, for didactic purposes, we limit our discussion in the main section using this framework. However, at cold temperatures the DIS approximation fails and we resort to a multichannel description involving all 16 channel states that describe the various hyperfine levels of the diatom system. That discussion is left for the Appendix and parallels the treatment in the main section. In addition, we include more traditional derivations in the Appendix of the close coupling equations to that described earlier. We show how the different formulations lead to the same description.

In Sec. III we report the final results that of all spin-changing cross sections for the H-H, H-T, and T-T systems for collision energies (gas temperatures) 1 mK $< E <$ 290 K. We show that the T-T system has a spin-exchange cross section that is more than 10^3 larger than the corresponding H-H cross section at 1 mK. We provide a brief summary and conclusion, unless otherwise stated atomic units will be used throughout.

II. THEORETICAL FRAMEWORK

Consider the ket $|F_a\, M_a\rangle$, where $F_a\, M_a$ are, respectively, the total and azimuthal hyperfine quantum numbers for hydrogen atom a in its ground state. In the asymptotic region, where atoms a and b are well separated, the direct product ket $|F_a\, M_a\, F_b\, M_b\rangle$ describes the quantum state of both atoms. If we neglect the small 1420 MHz ground-state hyperfine-energy defect between the $F = 1$ and 0 levels, the so-called DIS, or elastic approximation, we can describe the system in the $|S\, M_S\, I\, M_I\rangle$ representation, where $S = S_a + S_b$ is the total electronic spin angular momentum quantum number of the two atoms, $I = I_a + I_b$ is the total nuclear spin angular momentum number, and M_S and M_I are the quantum numbers for the corresponding azimuthal components. The relationships between the various representations in the scattering formalism are described in detail in Ref. [9].

The effective Hamiltonian for a pair of ground-state hydrogen atoms is given by

$$H = H_{\rm KE} + H_{\rm ad} + H_{\rm dip} + H_{\rm hf}, \tag{1}$$

where $H_{\rm KE}$ is the kinetic energy of relative motion and the adiabatic term

$$H_{AD} = [{}^3\Sigma(R) - {}^1\Sigma(R)]\boldsymbol{S}_a \cdot \boldsymbol{S}_b + \frac{3\,{}^3\Sigma(R) + {}^1\Sigma(R)}{4}, \tag{2}$$

where ${}^3\Sigma(R) \equiv b\,{}^3\Sigma_u^+(R)$ and ${}^1\Sigma(R) \equiv X\,{}^1\Sigma_g^+(R)$ are, respectively, the ground-state triplet and singlet BO potential curves for the H-H system expressed as a function of the radial separation distance $R = |\boldsymbol{R}|$. $\boldsymbol{S}_a$ and $\boldsymbol{S}_b$ are the electronic spin operators for atoms a and b, respectively.

$H_{\rm dip}$ is the long-range dipole magnetic electron spin-spin interaction (Breit interaction) between the pair of atoms [21]

$$H_{DIP} = \frac{\alpha^2}{R^3}\left[\boldsymbol{S}_a \cdot \boldsymbol{S}_b - 3\frac{(\boldsymbol{S}_a \cdot \boldsymbol{R})(\boldsymbol{S}_b \cdot \boldsymbol{R})}{R^2}\right], \tag{3}$$

where α is the fine-structure constant. We ignore interactions involving the nuclear spin angular momenta, which is justified by noting that the magnetic moment of the nuclei are on the order of 10^{-3} to that of the electrons. $H_{\rm hf}$ is the hyperfine interaction.

Significant simplification of the coupled scattering equations is achieved using the DIS approximation (i.e., we neglect $H_{\rm hf}$) and since we also ignore the nuclear-electron spin couplings, we can use molecular basis channel states that correlate in the asymptotic region to $|S\, M_S\, I\, M_I\rangle$. Following the method outlined in Ref. [22], we arrive at a set of coupled equations for the scattering amplitude $F_{SM_S}(\boldsymbol{R})$

$$\nabla^2 F_{SM_S}(\boldsymbol{R}) - 2\mu \sum_{S'M_S'} V_{SM_S}^{S'M_S'}(R,\theta,\phi) F_{S'M_S'}(\boldsymbol{R}) + k^2 F_{SM_S}(\boldsymbol{R}) = 0, \tag{4}$$

where μ is the nuclear-reduced mass of the collision system, $k = \sqrt{2\mu E}$ is the wave number for collision energy E, and the multichannel potential matrix is given by the expression (see the Appendix for derivations of the following)

$$V_{SM_S}^{S'M_S'}(\boldsymbol{R}) = \delta_{S,S'} \sum_{\Omega} \mathcal{D}^S_{M_S\Omega}(\phi,\theta,-\phi)\, \mathcal{D}^S_{\Omega M_{S'}}(\phi,-\theta,-\phi)\, \epsilon_{S\Omega}(R), \tag{5}$$

where $\epsilon_{S\Omega}(R)$ are the BO energy eigenvalues for the Hamiltonian $V \equiv H_{\rm ad} + H_{\rm dip}$. For the sake of economy in notation, we ignored the channel indices corresponding to the nuclear angular momenta, but take for granted that the potential matrix is multiplied by the factor $\delta_{I,I'}\delta_{M_I,M_{I'}}$.

The BO eigenvalues for V are given by the expressions (see Appendix)

$$\begin{aligned} \epsilon_{S=1,M_S} &= {}^3\Sigma(R) - \frac{\alpha^2}{2R^3} \quad |M_S| = 1, \\ \epsilon_{S=1,M_S} &= {}^3\Sigma(R) + \frac{\alpha^2}{R^3} \quad M_S = 0, \\ \epsilon_{S=0,M_S} &= {}^1\Sigma(R). \end{aligned} \tag{6}$$

Inserting the BO eigen-energies into Eq. (5) and using the unitarity property

$$\sum_{\Omega} \mathcal{D}^S_{M_S\Omega}(\phi,\theta,-\phi)\, \mathcal{D}^S_{\Omega M_{S'}}(\phi,-\theta,-\phi) = \delta_{M_S,M_{S'}}. \tag{7}$$

We obtain

$$\underline{V}(\boldsymbol{R}) = \begin{pmatrix} {}^3\Sigma(R) - \frac{\alpha^2[3\cos(2\theta)+1]}{8R^3} & -\frac{3e^{-i\phi}\alpha^2\sin(2\theta)}{4\sqrt{2}R^3} & -\frac{3e^{-2i\phi}\alpha^2\sin^2(\theta)}{4R^3} & 0 \\ -\frac{3e^{i\phi}\alpha^2\sin(2\theta)}{4\sqrt{2}R^3} & {}^3\Sigma(R) + \frac{[3\cos(2\theta)+1]\alpha^2}{4R^3} & \frac{3e^{-i\phi}\alpha^2\sin(2\theta)}{4\sqrt{2}R^3} & 0 \\ -\frac{3e^{2i\phi}\alpha^2\sin^2(\theta)}{4R^3} & \frac{3e^{i\phi}\alpha^2\sin(2\theta)}{4\sqrt{2}R^3} & {}^3\Sigma(R) - \frac{\alpha^2[3\cos(2\theta)+1]}{8R^3} & 0 \\ 0 & 0 & 0 & {}^1\Sigma(R) \end{pmatrix}. \tag{8}$$

Here, we expressed $V_{SM_S}^{S'M_{S'}}$ in matrix form and channel (column or row index) 1 refers to the $|S=1\ M_S=1\rangle$ state, channel 2 to the $|S=1 M_S=0\rangle$ state, channel 3 to the $|S=1\ M_S=-1\rangle$ state, and channel 4 to the $|S=0\ M_S=0\rangle$ state. Typically, one expands the multichannel scattering amplitude $F_{SM_S}(\boldsymbol{R})$ as a sum of partial waves. However, as a result of the anisotropy in $\underline{V}(\boldsymbol{R})$, the resulting scattering equations involve couplings between waves with different orbital angular momenta. At higher collision energies, where many partial waves contribute, the increased complexity requires significant CPU resources in propagating the numerical solution. Instead, we follow a procedure outlined in Ref. [22] where the amplitudes are expressed in the form

$$F_{SM_S}(\boldsymbol{R}) = \sum_{lm}\sum_{JM} Y_{lm}(\theta\phi)\sqrt{2J+1}\begin{pmatrix} S & l & J \\ M_S & m & -M \end{pmatrix}\frac{G_{Sl}^{JM}(R)}{R}, \tag{9}$$

and which lead to the following coupled radial equations

$$\frac{d^2\underline{G}^{JM}(R)}{dR^2} - \frac{\underline{L}(\underline{L}+1)}{R^2}\underline{G}^{JM}(R) - 2\mu\underline{W}\,\underline{G}^{JM}(R) + k^2\underline{G}^{JM}(R) = 0. \tag{10}$$

$\underline{G}^{JM}(R)$ is the multichannel radial scattering function, $\underline{L}$ is a diagonal matrix the entries of which are the channel orbital angular momenta, and $\underline{W}(R)$ is the multichannel radial potential matrix. The channel assignments for the radial equations are given in Table I, and in this representation the explicit form for the radial potential is given by

$$\underline{W}(R) = \begin{pmatrix} {}^3\Sigma(R) + \frac{(J-1)\alpha^2}{2(2J+1)R^3} & -\frac{3}{2}\frac{\sqrt{J(J+1)}\alpha^2}{(2J+1)R^3} & 0 & 0 \\ -\frac{3}{2}\frac{\sqrt{J(J+1)}\alpha^2}{2(J+1)R^3} & {}^3\Sigma(R) + \frac{(J+2)\alpha^2}{2(2J+1)R^3} & 0 & 0 \\ 0 & 0 & {}^3\Sigma(R) - \frac{\alpha^2}{2R^3} & 0 \\ 0 & 0 & 0 & {}^1\Sigma(R) \end{pmatrix}. \tag{11}$$

The solution of Eq. (10) for each partial wave $J\,M$ allows the determination of the scattering matrix and the desired scattering cross sections. One advantage of solving the system of equations in Eq. (10) is that they are block diagonal in the partial wave quantum numbers $J\,M$. This contrasts with alternate formulations in which an infinite array of radial partial wave functions are coupled and which requires demanding CPU and memory resources in their solution. In block diagonal form, embarrassingly parrallel methods can be exploited in their solution.

TABLE I. Channel quantum numbers for block J.

Channel	l	S
1	$J-1$	1
2	$J+1$	1
3	J	1
4	J	0

III. SCATTERING AMPLITUDE

In solving Eq. (10) we can construct the scattering amplitude as discussed in the following. We define the radial amplitude

$$\underline{G}^{JM}(R) \equiv G_{Sl}^{S'l'}(JM, R), \tag{12}$$

where the subscripts and superscripts on the right-hand side refer to incoming and outgoing channel indices as described in Table I. We enforce the boundary condition

$$G_{Sl}^{S'l'}(JM, R) \to \frac{\delta_{Sl}^{S'l'}}{k^{1/2}}\exp(-ikR)i^l - \frac{\exp(ikR)}{k^{1/2}}(-i)^l\mathcal{S}_{Sl}^{S'l'}(JM), \tag{13}$$

in the asymptotic limit, $R\to\infty$. Here $\mathcal{S}_{Sl}^{S'l'}(JM)$ is the radial S matrix for partial wave $J\,M$. Defining the amplitude

$$G_{m_a m_b}^{m_a' m_b'}(\boldsymbol{R}) \equiv \sum_{JM}\sum_{S,S'}\sum_{M_S,M_S'}\sum_{lm}\sum_{l'm'}\begin{pmatrix} S & l & J \\ M_S & m & -M \end{pmatrix} \times \begin{pmatrix} S' & l' & J \\ M_S' & m' & -M \end{pmatrix}[J][S,S']^{1/2}$$

$$\times Y_{lm}(\theta\phi)Y^*_{l'm'}(\theta_i\phi_i)\begin{pmatrix}\frac{1}{2} & \frac{1}{2} & S\\ m_a & m_b & -M_S\end{pmatrix}\times\begin{pmatrix}\frac{1}{2} & \frac{1}{2} & S'\\ m'_a & m'_b & -M'_S\end{pmatrix}\frac{2\pi i^{l+1}}{k^{1/2}R}G^{S'l'}_{Sl}(JM,R), \tag{14}$$

we find, as $R\to\infty$

$$G^{m'_a m'_b}_{m_a m_b}(\boldsymbol{R})\to\exp(i\boldsymbol{kR})\delta^{m'_a m'_b}_{m_a m_b}+f^{m'_a m'_b}_{m_a m_b}(\theta\phi;\theta_i\phi_i)\frac{\exp(ikR)}{R}, \tag{15}$$

where

$$f^{m'_a m'_b}_{m_a m_b}(\theta\phi;\theta_i\phi_i)=\sum_{JM}\sum_{lm}\sum_{l'm'}\frac{2\pi i}{k}Y_{lm}(\theta\phi)Y^*_{l'm'}(\theta_i\phi_i)\times\mathcal{T}^{S'l'}_{Sl}(JM)[J]\sum_{S,S'}\sum_{M_S,M'_S}[S,S']\times\begin{pmatrix}\frac{1}{2} & \frac{1}{2} & S\\ m_a & m_b & -M_S\end{pmatrix}\begin{pmatrix}\frac{1}{2} & \frac{1}{2} & S'\\ m'_a & m'_b & -M'_S\end{pmatrix}\times\begin{pmatrix}S & l & J\\ M_S & m & -M\end{pmatrix}\begin{pmatrix}S' & l' & J\\ M'_S & m' & -M\end{pmatrix}$$

$$\mathcal{T}^{S'l'}_{Sl}(JM)\equiv\delta^{S'l'}_{Sl}-\mathcal{S}^{S'l'}_{Sl}(JM), \tag{16}$$

is the scattering amplitude for a pair of atoms, in internal state $|m_a m_b\rangle$, approaching in the solid angle centered at $\theta_i\phi_i$ to scatter into state $|m'_a m'_b\rangle$ and the solid angle centered at $\theta\phi$. We re-express

$$f^{m'_a m'_b}_{m_a m_b}(\theta\phi;\theta_i\phi_i)=\sum_{lm}\sum_{l'm'}Y_{lm}(\theta\phi)Y^*_{l'm'}(\theta_i\phi_i)\frac{2\pi i}{k}W^{m'_a m'_b}_{m_a m_b}(lm,l'm')$$

$$W^{m'_a m'_b}_{m_a m_b}(lm,l'm')\equiv\sum_{JM}\sum_{S,S'}\sum_{M_S,M'_S}\begin{pmatrix}\frac{1}{2} & \frac{1}{2} & S\\ m_a & m_b & -M_S\end{pmatrix}\begin{pmatrix}\frac{1}{2} & \frac{1}{2} & S'\\ m'_a & m'_b & -M'_S\end{pmatrix}\times\begin{pmatrix}S & l & J\\ M_S & m & -M\end{pmatrix}\begin{pmatrix}S' & l' & J\\ M'_S & m' & -M\end{pmatrix}\times[S,S']^{1/2}[J]\mathcal{T}^{S'l'}_{Sl}. \tag{17}$$

We define the cross section

$$\sigma(m_a m_b\to m'_a m'_b)\equiv\frac{1}{4\pi}\int d\hat{\boldsymbol{\Omega}}_i\int d\hat{\boldsymbol{\Omega}}\left|f^{m'_a m'_b}_{m_a m_b}(\theta\phi;\theta_i\phi_i)\right|^2=\frac{\pi}{k^2}\sum_{lm}\sum_{l'm'}|W^{m'_a m'_b}_{m_a m_b}(lm,l'm')|^2. \tag{18}$$

If we ignore the dipolar interaction (i.e., $\alpha=0$), Eq. (11) predicts that

$$\mathcal{T}^{S'l'}_{Sl}(JM)=\delta_{S,S'}\delta_{l,l'}\mathcal{T}(S,l)\qquad\mathcal{T}(S,l)\equiv\mathcal{T}^{Sl}_{Sl}(JM). \tag{19}$$

We make use of the fact that $\mathcal{T}$ is not an explicit function of JM [it depends on J through the implicit relationship between l,l', i.e., $l=l(J),l'=l'(J)$]. For a fixed value of l we can then contract

$$\sum_{JM}[J]\begin{pmatrix}S & l & J\\ M_S & m & -M\end{pmatrix}\begin{pmatrix}S & l & J\\ M'_S & m' & -M\end{pmatrix}=\delta_{m,m'}\delta_{M_S,M'_S}, \tag{20}$$

to obtain

$$\sigma(m_a m_b\to m'_a m'_b)=\frac{\pi}{k^2}\sum_l(2l+1)\left|W^{m'_a m'_b}_{m_a m_b}(l)\right|^2$$

$$W^{m'_a m'_b}_{m_a m_b}(l)=\sum_{SM_S}[S]\begin{pmatrix}\frac{1}{2} & \frac{1}{2} & S\\ m_a & m_b & -M_S\end{pmatrix}\times\begin{pmatrix}\frac{1}{2} & \frac{1}{2} & S\\ m'_a & m'_b & -M_S\end{pmatrix}\mathcal{T}(S,l). \tag{21}$$

This expression presents the familiar spin-exchange selection rule $m_a+m_b=m'_a+m'_b$.

Using Eq. (21), we obtain

$$\sigma\left(\frac{1}{2}\,\frac{-1}{2}\Leftrightarrow\frac{1}{2}\,\frac{-1}{2}\right)=\frac{\pi}{2k^2}\sum_l(2l+1)\{3-2\cos(2\delta_{sl})-2\cos(2\delta_{tl})+\cos[2(\delta_{sl}-\delta_{tl})]\}$$

$$\sigma\left(\frac{1}{2}\,\frac{-1}{2}\Leftrightarrow\frac{-1}{2}\,\frac{1}{2}\right)=\frac{\pi}{k^2}\sum_l(2l+1)\,\sin^2(\delta_{sl}-\delta_{tl})$$

$$\sigma\left(\pm\frac{1}{2}\pm\frac{1}{2}\to\pm\frac{1}{2}\pm\frac{1}{2}\right)=\frac{4\pi}{k^2}\sum_l(2l+1)\,\sin^2(\delta_{tl}), \tag{22}$$

where $\mathcal{T}(S,l)=1-\exp[2i\delta_S(l)]$ and $\delta_S(l)$ is the lth partial wave phase shift for elastic scattering in the singlet ($S=0$) and ($S=1$) triplet BO potentials, respectively.

We also define the amplitude

$$G^{F'_a M'_a F'_b M'_b}_{F_a M_a F_b M_b}(\boldsymbol{R})\equiv\sum_{JM}\sum_{lm}\sum_{l'm'}\sum_{IM_I}\sum_{S,S'}\sum_{M_S,M'_S}\times[J][S,S']\langle F_a M_a F_b M_b|IM_I SM_S\rangle\times\begin{pmatrix}S & l & J\\ M_S & m & -M\end{pmatrix}\begin{pmatrix}S' & l' & J\\ M'_S & m' & -M\end{pmatrix}\times\langle S'M'_S IM_I|F'_a M'_a F'_b M'_b\rangle Y_{lm}(\theta\phi)Y^*_{l'm'}(\theta_i\phi_i)\frac{2\pi i^{l+1}}{k^{1/2}R}G^{S'l'}_{Sl}(JM,R), \tag{23}$$

which has the asymptotic limit

$$G^{F'_a M'_a F'_b M'_b}_{F_a M_a F_b M_b}(\boldsymbol{R})\to\exp(i\boldsymbol{kR})\delta^{F'_a M'_a F'_b M'_b}_{F_a M_a F_b M_b}+f^{F'_a M'_a F'_b M'_b}_{F_a M_a F_b M_b}(\theta\phi;\theta_i\phi_i)\frac{\exp(ikR)}{R}, \tag{24}$$

where

$$f^{F'_a M'_a F'_b M'_b}_{F_a M_a F_b M_b}(\theta\phi;\theta_i\phi_i)=\sum_{lm}\sum_{l'm'}Y_{lm}(\theta\phi)Y^*_{l'm'}(\theta_i\phi_i)\frac{2\pi i}{k}W^{F'_a M'_a F'_b M'_b}_{F_a M_a F_b M_b}(lm;l'm'), \tag{25}$$

$$W^{F_a' M_a' F_b' M_b'}_{F_a M_a F_b M_b}(lm; l'm') = \sum_{JM}\sum_{IM_I}\sum_{S,S'}\sum_{M_S,M_S'}[J][S,S']\mathcal{T}^{S'l'}_{Sl}\langle F_a M_a F_b M_b|IM_I SM_S\rangle \times \begin{pmatrix} S & l & J \\ M_S & m & -M \end{pmatrix}\begin{pmatrix} S' & l' & J \\ M_S' & m' & -M \end{pmatrix} \times \langle S'M_S' IM_I|F_a' M_a' F_b' M_b'\rangle, \quad (26)$$

and

$$\langle SM_S IM_I|F_a M_a F_b M_b\rangle = \sum_{FM_F}(-1)^{F_b-F_a+F}[F][F_a,F_b,S,I]^{1/2} \times \begin{pmatrix} F_a & F_b & F \\ M_a & M_b & -M \end{pmatrix}\begin{pmatrix} S & F & I \\ M_S & -M_F & -M_I \end{pmatrix} \times \begin{Bmatrix} 1/2 & 1/2 & F_a \\ 1/2 & 1/2 & F_b \\ S & I & F \end{Bmatrix}. \quad (27)$$

Thus,

$$\sigma(F_a' M_a' F_b' M_b' \to F_a M_a F_b M_b) = \frac{1}{4\pi}\int d\hat{\mathbf{\Omega}}_i \int d\hat{\mathbf{\Omega}}\left|f^{F_a M_a F_b M_b}_{F_a' M_a' F_b' M_b'}(\theta\phi;\theta_i\phi_i))\right|^2 = \frac{\pi}{k^2}\sum_{lm}\sum_{l'm'}\left|W^{F_a' M_a' F_b' M_b'}_{F_a M_a F_b M_b}(lm,l'm')\right|^2. \quad (28)$$

Significant simplification is achieved if we ignore the anisotropic interaction so that Eq. (19) is true. Then we obtain

$$\sigma(F_a M_a F_b M_b \to F_a' M_a' F_b' M_b') = \frac{\pi}{k^2}\sum_l(2l+1)\left|W^{F_a' M_a' F_b' M_b'}_{F_a M_a F_b M_b}(l)\right|^2$$

$$W^{F_a' M_a' F_b' M_b'}_{F_a M_a F_b M_b}(l) = \sum_{IM_I}\sum_{SM_S}\mathcal{T}(S,l)\langle F_a M_a F_b M_b|IM_I SM_S\rangle \times\langle SM_S IM_I|F_a' M_a' F_b' M_b'\rangle. \quad (29)$$

Evaluating the recoupling unitary matrix Eq. (27) we obtain, for the nonvanishing off diagonal cross sections,

$$\sigma(F_a M_a F_b M_b \to F_a' M_a' F_b' M_b') = \frac{\pi}{4k^2}\sum_l(2l+1)\sin^2(\delta_{sl}-\delta_{tl}), \quad (30)$$

provided that the selection rule $M_a + M_b = M_a' + M_b'$ is met. We also find that the $F_a = 0\, F_b = 0 \Leftrightarrow F_a = 1 M_a = \pm 1\, F_b = 1 M_b = \mp 1$ cross sections vanish identically. Expression (30) was first derived by Dalgarno [6] within the elastic, or DIS, approximation.

A. Symmetry considerations

Because the electrons and protons in the collision of two hydrogen atoms are identical particles, we must impose the correct symmetries in the scattering wave functions, which is expressed as a sum of a product of multichannel amplitudes with channel states

$$\Psi = \sum_\gamma F_\gamma(\mathbf{R})|\gamma\rangle, \quad (31)$$

where the channel index γ refers either to the $|SM_S IM_I\rangle = |SM_S\rangle \otimes |IM_I\rangle$ or $|F_a M_a F_b M_b\rangle$ representations. Let P_e represent the electron permutation operator, then

$$P_e|SM_S\rangle = -|SM_S\rangle, \quad (32)$$

since $|SM_S\rangle$ is a product of the spatial ungerade and gerade electronic functions with the triplet and singlet spin states for $S = 1$ and $S = 0$, respectively. Also, the $|F_a M_a F_b M_b\rangle$ basis vectors are linear combinations of $|SM_s\rangle$ so they are also odd eigenstates of the total electron exchange operator. In the multichannel expansion electronic (spatial and spin), coordinates enter only through the basis functions. To properly account for nuclear permutation we need to understand the effect of the nuclear permutation operator P_n on both the channel basis and the scattering function. Now, since we are working in the atomic gauge [22]

$$P_n|SM_S\rangle = (-1)^S|SM_S\rangle$$
$$P_n|IM_I\rangle = (-1)^{I+1}|IM_I\rangle \quad (33)$$
$$P_n|SM_S IM_I\rangle = (-1)^{S+I+1}|SM_S IM_I\rangle.$$

Thus,

$$P_n|F_a M_a F_b M_b\rangle = \sum_{IM_I}\sum_{SM_S}\sum_{FM_F}(-1)^{F_b-F_a+F}[F][F_a,F_b,S,I]^{1/2} \times \begin{pmatrix} F_a & F_b & F \\ M_a & M_b & -M \end{pmatrix}\begin{pmatrix} S & F & I \\ M_S & -M_F & -M_I \end{pmatrix} \times \begin{Bmatrix} 1/2 & 1/2 & F_a \\ 1/2 & 1/2 & F_b \\ S & I & F \end{Bmatrix}(-1)^{S+I+1}|SM_S IM_I\rangle, \quad (34)$$

where we used Eqs. (33) and (27).

Because

$$\begin{Bmatrix} 1/2 & 1/2 & F_a \\ 1/2 & 1/2 & F_b \\ S & I & F \end{Bmatrix} = (-1)^{F_a+F_b+I+S+F}\begin{Bmatrix} 1/2 & 1/2 & F_b \\ 1/2 & 1/2 & F_a \\ S & I & F \end{Bmatrix}, \quad (35)$$

$$\begin{pmatrix} F_a & F_b & F \\ M_a & M_b & -M \end{pmatrix} = (-1)^{F_a+F_b+F}\begin{pmatrix} F_b & F_a & F \\ M_b & M_a & -M \end{pmatrix}, \quad (36)$$

and the fact that F_a, F_b, S, and I are integers, we obtain

$$P_n|F_a M_a F_b M_b\rangle = -|F_b M_b F_a M_a\rangle. \quad (37)$$

According to Eq. (37) we require $F_{F_a M_a F_b M_b}(\boldsymbol{R}) = F_{F_b M_b F_a M_a}(-\boldsymbol{R})$ and proceeding as in Ref. [22], we generalize Eq. (23) to obtain

$$\sigma(F_a M_a F_b M_b \to F_a' M_a' F_b' M_b') = \frac{1}{4\pi}\int d\hat{\mathbf{\Omega}}_i \int d\hat{\mathbf{\Omega}}\frac{1}{2}\left|f^{F_a M_a F_b M_b}_{F_a' M_a' F_b' M_b'}(\theta\phi;\theta_i\phi_i) + f^{F_b M_b F_b M_b}_{F_a' M_a' F_b' M_b'}(\pi-\theta,\phi+\pi;\theta_i\phi_i)\right|^2$$

$$= \frac{\pi}{2k^2} \sum_{lm} \sum_{l'm'} \left| W^{F'_a M'_a F'_b M'_b}_{F_a M_a F_b M_b}(lm, l'm') + (-1)^l W^{F'_a M'_a F'_b M'_b}_{F_b M_b F_a M_a}(lm, l'm') \right|^2. \quad (38)$$

For the special case when the anisotropic interaction is ignored, expression (38) reduces to

$$\sigma(F_a M_a F_b M_b \to F'_a M'_a F'_b M'_b) = \sigma^{\pm} = \frac{\pi}{2k^2} \sum_{l\pm} (2l+1) \sin^2(\delta_{sl} - \delta_{tl}), \quad (39)$$

where $l\pm$ refers to even and odd values for l, respectively. For $|F_a + F_b - F'_a - F'_b| = 0,\ 2$, $\sigma(F_a M_a F_b M_b \to F'_a M'_a F'_b M'_b) = \sigma^+$ and for $|F_a + F_b - F'_a - F'_b| = 1$, $\sigma(F_a M_a F_b M_b \to F'_a M'_a F'_b M'_b) = \sigma^-$. The cross sections for the $F_a = 0\, F_b = 0 \Leftrightarrow F_a = 1 M_a = \pm 1\, F_b = 1 M_b = \mp 1$ transitions vanish identically.

IV. RESULTS AND DISCUSSION

In Fig. 1 we present the $\Delta M = \pm 1, \pm 2$ transition cross sections as functions of collision energies 1 mK $< E <$ 290 K, expressed in units of Kelvin. The cross sections are itemized,

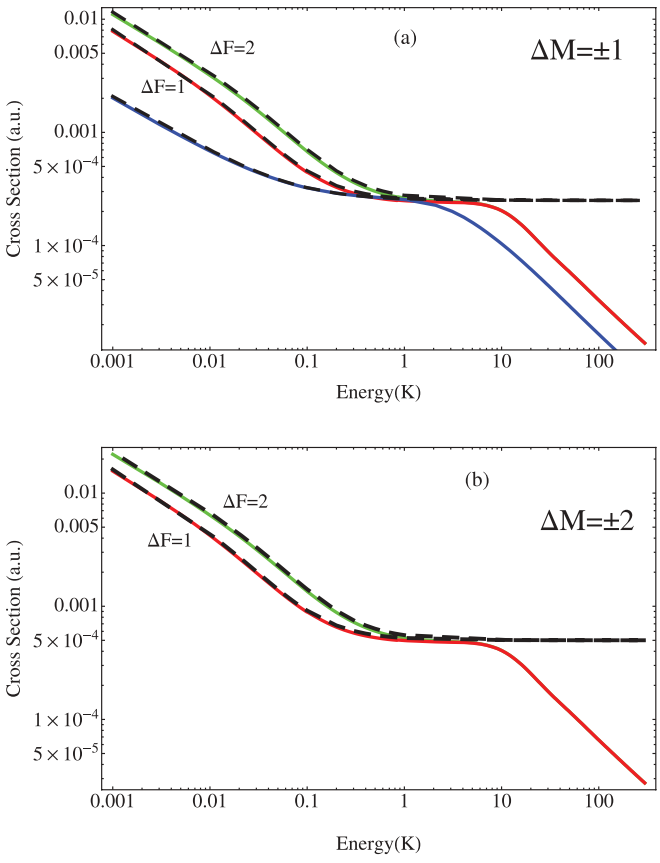

FIG. 1. (Color online) (a) Solid lines represent results for the multichannel calculation of hyperfine level quenching cross sections for the H-H system corresponding to $\Delta M = \pm 1$ transitions. The dashed lines represent results obtained using the Born approximation. (b) Solid lines represent results for the multichannel calculation of hyperfine level quenching cross sections for the H-H system corresponding to $\Delta M = \pm 2$ transitions. The dashed lines represent results obtained using the Born approximation.

in addition to the change in azimuthal spin angular momentum M, by the change in the diatom total hyperfine quantum number. We define $\Delta F \equiv F_a + F_b - F'_a - F'_b$, where F_a is the initial hyperfine quantum number of atom a and F'_a its final hyperfine quantum number. In that figure the lines labeled $\Delta F = 2$ correspond to transitions where $F_a = F_b = 1$ and $F'_a = F'_b = 0$ and $\Delta F = 1$ to transitions where $F_a = F_b = 1$ and one of the other atoms is in the ground hyperfine level. $\Delta M \neq 0$ quenching cross sections, corresponding to transitions in which only one of the atoms is initially in its $F = 1$ state are null.

The dashed lines in the figure correspond to the results of calculations performed within the Born approximation. We find that the latter provide an excellent description at lower collision energies $\approx <$ 1 K. The success of the Born approximation is a consequence of two properties of this system. The magnetic interactions are very small, proportional to α^2, and due to its long-range nature, transitions are driven by it in the asymptotic region [18]. At higher collision energies we find that the results of the multichannel cross sections exhibit a monotonic decrease, whereas the Born approximation predicts cross sections that tend to a constant value [see Eq. (D6)]. This is a consequence of the $1/R^3$ behavior of the magnetic interactions and leads to an overestimation by the Born approximation of contributions from the region $R \to 0$ [23]. The inner repulsive wall of the $b\,^3\Sigma_u$ potential restricts close atom encounters and, as a consequence, leads to monotonically decreasing cross sections at higher energies as shown in Fig. 1. For $\Delta M = \pm 1$, there exist two components for the $\Delta F = 1$ cross sections that are due to exchange symmetry requirements for the H-H system.

In Fig. 2 we present the results for the H-T collision system. Because this is a heteronuclear system exchange effects are not present here. The energy defect for the hyperfine transition energy is about 1% larger for tritium than for hydrogen and therefore the cross sections shown in Fig. 2 have several components at colder temperatures, however, those differences are too small to be resolved in that figure.

In Fig. 3 we present the results for the T-T collision system. There are qualitative similarities with the cross sections of the H-H and H-T systems. However, at lower energies the Born approximation fails to accurately predict the spin-flipping cross sections. According to Eq. (D6), the T-T cross sections should be a factor $(\mu_{\rm TT}/\mu_{\rm HH})^2 \approx 9$ larger than the corresponding H-H cross sections. Figure 3 illustrates that the cross sections are an order of magnitude larger than implied by this scaling. To understand this behavior we need to discuss the molecular parameters assumed in our calculations.

In our calculations we use the BO energies for the $b\,^3\Sigma_u^+$, $X\,^1\Sigma_g^+$ states of the H-H system, described in Ref. [24] and references therein. The *ab-initio* data are modified to include mass-dependent adiabatic corrections, relativistic corrections, and are fitted smoothly to the long-range dispersion energies [24]. In the present study we added more *ab-initio* potential data points, reported in Ref. [25], in our fitting program. With these potentials we find, for the H-H system, a scattering length $a_s = 0.45 a_0$ (we exclusively used the nuclear-reduced masses in the present calculations) for the singlet potential and $a_t = 1.31 a_0$ for the triplet potential. The latter value is a significant change from a previous calculated

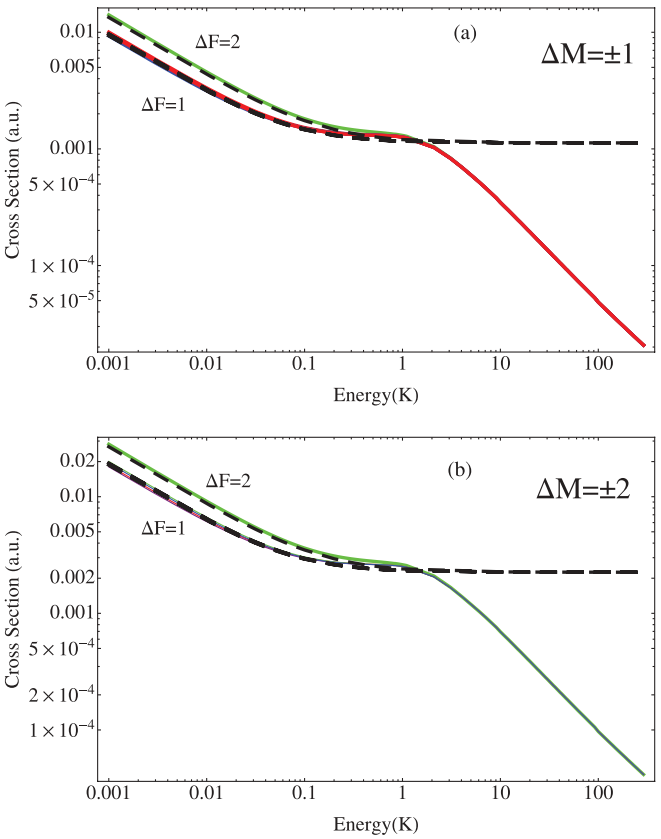

FIG. 2. (Color online) (a) Solid lines represent results for the multichannel calculation of hyperfine level quenching cross sections for the H-T system corresponding to $\Delta M = \pm 1$ transitions. The dashed lines represent results obtained using the Born approximation. (b) Solid lines represent results for the multichannel calculation of hyperfine level quenching cross sections for the H-T system corresponding to $\Delta M = \pm 2$ transitions. The dashed lines represent results obtained using the Born approximation.

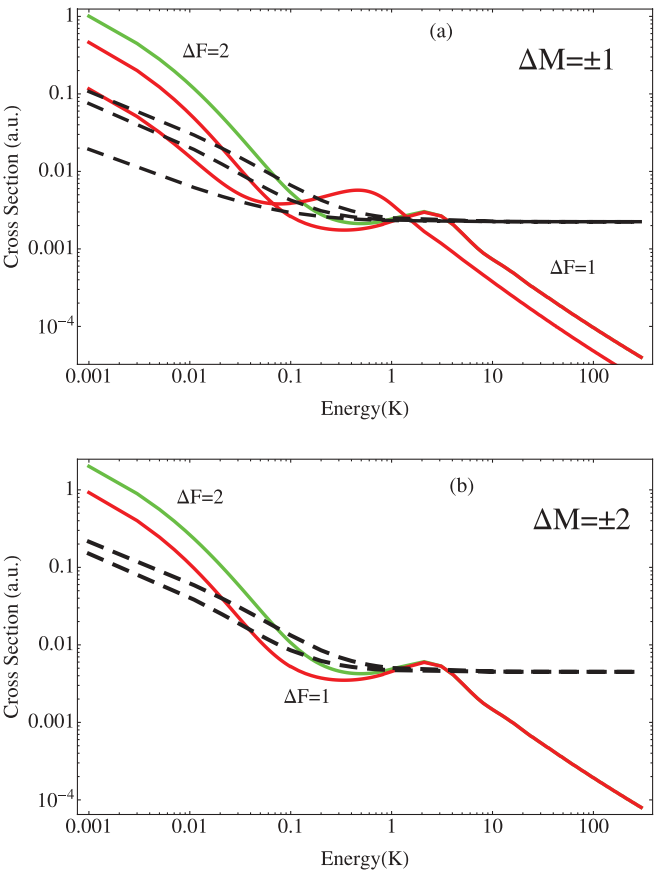

FIG. 3. (Color online) (a) Solid lines represent results for the multichannel calculation of hyperfine level quenching cross sections for the T-T system corresponding to $\Delta M = \pm 1$ transitions. The dashed lines represent results obtained using the Born approximation. (b) Solid lines represent results for the multichannel calculation of hyperfine level quenching cross sections for the T-T system corresponding to $\Delta M = \pm 2$ transitions. The dashed lines represent results obtained using the Born approximation.

value $a_t = 1.21a_0$ [24]. For the H-T and T-T systems we mass scale the adiabatic corrections, but do not include mass dependent nonadiabatic corrections [26] for the heteronuclear H-T system. The latter were calculated for the H-D system and were shown to give a small correction to the scattering length of the singlet potential [26] in that system. For the tritium dimer we find $a_s = 33.4a_0$ and $a_t = -87.9a_0$. The large negative value for the triplet scattering length implies the existence of a nascent bound level for the $b\,^3\Sigma_u^+$ state of the tritium dimer [27]. Because perturbative methods fail to accurately account for resonance or threshold phenomena, the presence of this virtual state contributes to the breakdown of the Born approximation at lower collision energies.

Evidence for a threshold resonance effect is also evident by inspection of the $\Delta M = 0$, or spin exchange, cross sections shown in Fig. 4. In the top panel of that figure we present data for the $\Delta F = 2$ transitions. The solid lines represent data obtained by the multichannel calculations, whereas the dashed lines represent data obtained in the elastic approximation and for homonuclear systems is given by [10] [see also Eq. (39)]

$$\sigma_+ = \frac{\pi}{2k^2} \sum_{l\ \text{even}} (2l+1) \sin^2(\delta_{sl} - \delta_{tl}). \tag{40}$$

In the limit $k \to 0$, expression (40) predicts that the cross sections tend to a constant

$$\sigma_+ \to \frac{\pi}{2} |a_t - a_s|^2, \tag{41}$$

where a_t and a_s are, respectively, the triplet and singlet scattering lengths. This behavior is exhibited in Fig. 4 by the H-H and H-T cross sections obtained with the elastic approximation. For the T-T system, this limiting behavior becomes apparent at energies ≈1 mK. Using the values for the T-T scattering lengths given earlier, the elastic approximation predicts $\sigma_+ \approx 2.3 \times 10^4 a_0^2$ close to the value obtained in the multichannel calculation at 1 mK. The large cross section is a consequence of the large, negative, scattering length due to the nascent bound level. Of course, the elastic approximation does not predict the correct Wigner threshold behavior in the ultracold limit. For inelastic transitions the latter requires that cross sections increase in proportion to $1/k$ as $k \to 0$. The correct Wigner threshold behavior is evident in the multichannel cross sections show in Fig. 4(a). In panel (b) we illustrate $\Delta F = 1$ spin-exchange cross sections and in the elastic approximation they are given, for H-H and T-T,

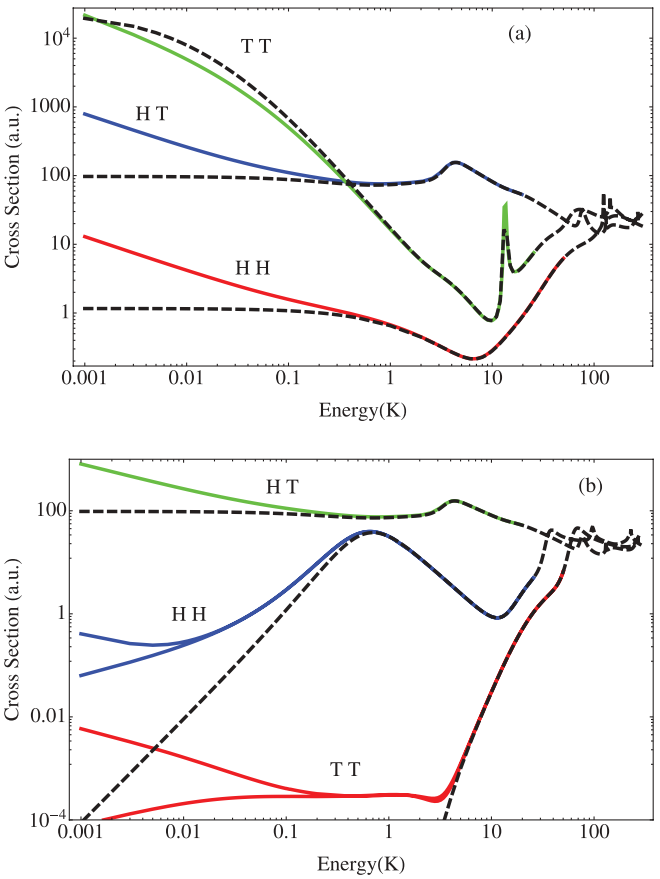

FIG. 4. (Color online) (a) Solid lines represent results for the multichannel calculation of $\Delta F = 2$ spin-exchange cross sections, the dashed lines represent results obtained using Eq. (40). (b) Solid lines represent results for the multichannel calculation of $\Delta F = 1$ spin-exchange cross sections, the dashed lines represent results obtained using Eq. (41).

by [10]

$$\sigma_- = \frac{\pi}{2k^2}\sum_{l\ \mathrm{odd}}(2l+1)\sin^2(\delta_{sl}-\delta_{tl}). \tag{42}$$

The restriction that only odd partial waves contribute to σ_- leads to the monotonic decrease in the cross sections as $k \to 0$. Because of close coupling effects and the dipolar interaction, this behavior is not necessarily exhibited by the cross section data obtained within the multichannel theory. For the H-T system, the elastic approximation cross sections are given by Eq. (30) and as $k \to 0$ the $\Delta F = 2$ and 1 cross sections have the same limit in this approximation. In Figs. 4(a) and (b) the two H-T multichannel cross sections both exhibit Wigner threshold behavior.

In summary, we introduce a multichannel molecular scattering theory in which electrostatic and magnetic interactions are treated on equal footing in the BO separation of the electronic and scattering coordinates. The latter interactions split the $b\,^3\Sigma_u$ energies and it is shown here how that leads to spin-flipping ($\Delta M \neq 0$) transitions in collisions of hydrogen atoms. We apply the theory to calculate all spin-changing processes in collisions of H with H, H with T, and T with T, and compared the results of the multichannel calculations with those predicted by the Born approximation and the elastic approximation. We show how the presence of a virtual, nascent, bound level supported by the $b\,^3\Sigma_u$ BO molecular potential leads to enhanced spin-exchange and spin-flip cross sections for the tritium dimer.

ACKNOWLEDGMENTS

This work was supported by NSF Grant No. PHY-0758140 and, in part, by a NASA EPSCoR grant given to the state of Nevada and DE-FG36-05GO85028. I would like to thank A. Dalgarno, J. Babb and T. Tscherbul for useful discussions.

APPENDIX A: METHOD A

A general expression for the effective anisotropic multichannel potential for two atoms with electronic angular momenta j_a and j_b is given in Ref. [22]. Because we are here considering only S-state atoms, we can generalize that theory to include hyperfine structure. Proceedings along the lines leading to Eq. (58) in Ref. [22], we obtain the following expression for the anisotropic potential,

$$\begin{aligned}\underline{V}(R\theta\phi) = &\sum_{IM_I}\sum_{SM_S}\sum_{\Omega}[F,F',F_a,F_a',F_b,F_b']^{1/2}[S,I]\\ &\times \mathcal{D}^{F'}_{M_F'\Omega}(\phi,\theta,-\phi)\,\mathcal{D}^{F}_{\Omega M_F}(\phi,-\theta,-\phi)\\ &\times \begin{pmatrix} I & S & F\\ M_I & M_S & -\Omega\end{pmatrix}\begin{pmatrix} I & S & F'\\ M_I & M_S & -\Omega\end{pmatrix}\\ &\times \begin{Bmatrix} 1/2 & I_a & F_a\\ 1/2 & I_b & F_b\\ S & I & F\end{Bmatrix}\begin{Bmatrix} 1/2 & I_a & F_a'\\ 1/2 & I_b & F_b'\\ S & I & F'\end{Bmatrix}\epsilon_{S M_S}(R),\end{aligned} \tag{A1}$$

where F is the total atom-atom spin angular momentum, F_a and F_b are the hyperfine quantum numbers for atoms a and b respectively, and I_a and I_b are the quantum numbers for nuclear spin.

$$\begin{aligned}&\mathcal{D}^{j}_{\Omega,\Omega'}(\phi,\theta,-\phi)\\ &\quad\equiv \langle j\Omega|\exp(-i\phi \boldsymbol{j}_z)\exp(-i\theta \boldsymbol{j}_y)\exp(i\phi \boldsymbol{j}_z)|j\Omega'\rangle,\end{aligned} \tag{A2}$$

is a Wigner rotation matrix and $\epsilon_{S\Omega}(R)$ are the BO eigenvalues for Hamiltonian $H_{\mathrm{ad}} + H_{\mathrm{dip}}$. The anisotropy of H_{dip} leads to a dependence of the BO eigenvalues on the azimuthal quantum number Ω. We apply a partial wave expansion for the multichannel amplitudes that are described in detail in Ref. [22]. With channel indices now specified by quantum numbers F, l, F_a, and F_b, we obtain the multichannel radial equation Eq. (10), for a given partial wave $J\,M$, with the potential matrix given by

$$\begin{aligned}&V^{F l F_a F_b}_{F' l' F_a' F_b'}(R)\\ &\quad= \sum_{IM_I}\sum_{SM_S}\sum_{\Omega}[F,F',F_a,F_a',F_b,F_b',l,l']^{1/2}[S,I]\\ &\qquad\times \begin{pmatrix} I & S & F\\ M_I & M_S & -\Omega\end{pmatrix}\begin{pmatrix} I & S & F'\\ M_I & M_S & -\Omega\end{pmatrix}\end{aligned}$$

$$\times \begin{pmatrix} F & l & J \\ \Omega & 0 & -\Omega \end{pmatrix} \begin{pmatrix} F' & l' & J \\ \Omega & 0 & -\Omega \end{pmatrix} \times \begin{Bmatrix} 1/2 & I_a & F_a \\ 1/2 & I_b & F_b \\ S & I & F \end{Bmatrix} \begin{Bmatrix} 1/2 & I_a & F'_a \\ 1/2 & I_b & F'_b \\ S & I & F' \end{Bmatrix} \epsilon_{S M_S}(R). \quad \text{(A3)}$$

Suppose $I_a = 0$ and $I_b = 0$ (i.e., $F \to S$) then

$$\begin{Bmatrix} 1/2 & 0 & F_a \\ 1/2 & 0 & F_b \\ S & 0 & F \end{Bmatrix} \to \frac{\delta_{F_a,1/2}\delta_{F_b,1/2}\delta_{S,F}}{[F_a, F_b, F]^{1/2}}, \quad \text{(A4)}$$

$I = 0$,

$$\begin{pmatrix} 0 & S & F \\ 0 & M_S & -\Omega \end{pmatrix} = (-1)^{S-\Omega} \frac{\delta_{\Omega,M_S}\delta_{S,F}}{[S]^{1/2}}, \quad \text{(A5)}$$

and expression (A3) reduces to

$$\underline{V}(R) = \delta_{S,S'} \sum_{\Omega} [l, l']^{1/2} \begin{pmatrix} S & l & J \\ \Omega & 0 & -\Omega \end{pmatrix} \times \begin{pmatrix} S' & l' & J \\ \Omega & 0 & -\Omega \end{pmatrix} \epsilon_{S\Omega}(R). \quad \text{(A6)}$$

Equation (A6) is consistent with the expression obtained in the direct product $|SM_S I M_I\rangle$ representation. Using the quantum number entries in Table I and the BO eigenvalues in Eq. (6), we obtain the radial potential matrix given by Eq. (11).

APPENDIX B: METHOD B

In this section we provide an alternative derivation of Eqs. (4) and (5). Recognizing that the H-H collision system comprises a two-qubit logic gate, we formulate this description in the language of quantum information theory [28].

We define the so-called computational basis [28] as the direct product $|m_a\rangle|m_b\rangle$, where m_a and m_b are the azimuthal components of electronic spin for atoms a and b, respectively, defined with respect to the inertial laboratory frame z axis. Following convention [28] the basis kets are labeled as two-qubit states

$$\begin{aligned} |1\rangle &= \left|\tfrac{-1}{2}\ \tfrac{-1}{2}\right\rangle \equiv |00\rangle, \\ |2\rangle &= \left|\tfrac{-1}{2}\ \tfrac{1}{2}\right\rangle \equiv |01\rangle, \\ |3\rangle &= \left|\tfrac{1}{2}\ \tfrac{-1}{2}\right\rangle \equiv |10\rangle, \\ |4\rangle &= \left|\tfrac{1}{2}\ \tfrac{1}{2}\right\rangle \equiv |11\rangle. \end{aligned} \quad \text{(B1)}$$

In this basis we find that

$$V \equiv H_{\rm ad} + H_{\rm dip} = U Z^\dagger H_{\rm BO} Z U^\dagger, \quad \text{(B2)}$$

where U is a two-qubit gate (unitary transformation) defined as the direct product

$$U_a \otimes U_b = \begin{pmatrix} \cos\left(\frac{\theta}{2}\right) & -e^{i\phi}\sin\left(\frac{\theta}{2}\right) \\ e^{-i\phi}\sin\left(\frac{\theta}{2}\right) & \cos\left(\frac{\theta}{2}\right) \end{pmatrix}_a \otimes \begin{pmatrix} \cos\left(\frac{\theta}{2}\right) & -e^{i\phi}\sin\left(\frac{\theta}{2}\right) \\ e^{-i\phi}\sin\left(\frac{\theta}{2}\right) & \cos\left(\frac{\theta}{2}\right) \end{pmatrix}_b, \quad \text{(B3)}$$

Z is the two-qubit gate

$$Z = \begin{pmatrix} 0 & 0 & 0 & 1 \\ 0 & \frac{-1}{\sqrt{2}} & \frac{-1}{\sqrt{2}} & 0 \\ 1 & 0 & 0 & 0 \\ 0 & -\frac{1}{\sqrt{2}} & \frac{1}{\sqrt{2}} & 0 \end{pmatrix}, \quad \text{(B4)}$$

and

$$H_{\rm BO} = \begin{pmatrix} {}^3\Sigma(R) - \frac{\alpha^2}{2R^3} & 0 & 0 & 0 \\ 0 & {}^3\Sigma(R) + \frac{\alpha^2}{R^3} & 0 & 0 \\ 0 & 0 & {}^3\Sigma(R) - \frac{\alpha^2}{2R^3} & 0 \\ 0 & 0 & 0 & {}^1\Sigma(R) \end{pmatrix}. \quad \text{(B5)}$$

We consider the new Hamiltonian

$$V' \equiv ZVZ^\dagger = \begin{pmatrix} {}^3\Sigma(R) - \frac{\alpha^2[3\cos(2\theta)+1]}{8R^3} & \frac{-3e^{-i\phi}\alpha^2\sin(2\theta)}{4\sqrt{2}R^3} & -\frac{3e^{-2i\phi}\alpha^2\sin^2(\theta)}{4R^3} & 0 \\ \frac{-3e^{i\phi}\alpha^2\sin(2\theta)}{4\sqrt{2}R^3} & {}^3\Sigma(R) + \frac{[3\cos(2\theta)+1]\alpha^2}{4R^3} & \frac{3e^{-i\phi}\alpha^2\sin(2\theta)}{4\sqrt{2}R^3} & 0 \\ \frac{-3e^{2i\phi}\alpha^2\sin^2(\theta)}{4R^3} & \frac{3e^{i\phi}\alpha^2\sin(2\theta)}{4\sqrt{2}R^3} & {}^3\Sigma(R) - \frac{\alpha^2[3\cos(2\theta)+1]}{8R^3} & 0 \\ 0 & 0 & 0 & {}^1\Sigma(R) \end{pmatrix}. \quad \text{(B6)}$$

$\underline{V}'$, expressed in the computational basis, has the same form as $\underline{V}$ in Eq. (8) expressed in the $|SM_S\rangle$ representation. The latter representation includes the Bell (entangled) states $|S = 1 M_S = 0\rangle$ and $|S = 0 M_S = 0\rangle$. The two representations are related via the Z gate defined earlier. We note that $H_{\rm BO}$ in Eq. (B5) is the Hamiltonian $H_{\rm ad} + H_{\rm dip}$ for the special case where the nuclear orientation is along the z axis of the laboratory frame ($\theta = 0, \phi = 0$) expressed in the $|SM\rangle$

basis. According to Eq. (B2) $\underline{V}$ is related to $H_{\rm BO}$ via a unitary transformation and so we can simply read off the eigenvalues (BO eigenvalues) of $\underline{V}$ from Eq. (B5)

$$\begin{aligned}\epsilon(S=1,M_S) &= {}^3\Sigma(R) - \frac{\alpha^2}{2R^3} \quad |M_S|=1\\ \epsilon(S=1,M_S) &= {}^3\Sigma(R) + \frac{\alpha^2}{R^3} \quad M_S=0\\ \epsilon(S=0,M_S) &= {}^1\Sigma(R).\end{aligned} \tag{B7}$$

APPENDIX C: METHOD C

In this section we utilize the Racah-algebra description used in previous studies [29,30] of collisions involving anisotropic, angular momentum-changing transitions. For the purpose of this discussion, we ignore the isotropic molecular interaction $H_{\rm ad}$. Typically, the scattering function in the DIS approximation can be expressed in the form

$$\begin{aligned}F(\mathbf{R}) &= \sum_{SM_S}\sum_{lm}\frac{F^{lm}_{SM_S}(R)}{R}Y_{lm}(\theta\phi)|SM_S\rangle\\ &\equiv \sum_{SM_S}\sum_{lm}\frac{F^{lm}_{SM_S}(R)}{R}|SM_S\,lm\rangle,\end{aligned} \tag{C1}$$

here $|SM_S\rangle$ is the channel basis vector for the pair of atoms described by the total spin S quantum number and its azimuthal projection M_S. $Y_{lm}(\theta\phi)$ are the spherical harmonics and $F^{lm}_{SM_S}(R)$ is the multichannel radial partial wave function for angular momenta l, m. When constructing the radial coupling equations this description leads to a coupling matrix given by

$$\underline{W} = \langle SM_S\,lm|H_{\rm dip}|S'M'_S\,l'm'\rangle. \tag{C2}$$

It is convenient to express $H_{\rm dip}$ as an irreducible tensor operator [29,30]

$$\begin{aligned}H_{\rm dip} &= v(R)\sum_q(-1)^q Y^{(2)}_q S^{(2)}_{-q} = v(R)\,Y^{(2)}\cdot S^{(2)},\\ v(R) &= -\sqrt{\frac{24\pi}{5}}\frac{\alpha^2}{R^3}.\end{aligned} \tag{C3}$$

Here $Y^{(2)}$ is the rank-2 tensor in configuration space $\theta\phi$ and $S^{(2)}$ is a rank-2 tensor in the product space of electronic spin. In the form given above, $H_{\rm dip}$ is therefore a rank-0 operator in the space that is spanned by the product of spin and configuration basis vectors. Therefore,

$$\begin{aligned}&\langle SM_S\,l\,m|H_{\rm dip}|S'M'_S\,l'm'\rangle\\ &= v(R)\sum_q\langle SM_S|S^{(2)}_{-q}|S'M_{S'}\rangle\langle lm|Y^{(2)}_q|l'm'\rangle\\ &= v(R)\sum_q(-1)^{S+l+q-M_S-m}\begin{pmatrix}S & 2 & S'\\ -M_S & -q & M'_S\end{pmatrix}\\ &\quad\times\begin{pmatrix}l & 2 & l'\\ -m & q & m'\end{pmatrix}\langle S||S^{(2)}||S'\rangle\langle l||Y^{(2)}||l'\rangle,\end{aligned} \tag{C4}$$

and

$$\langle l||Y^{(2)}||l'\rangle = (-1)^l[l,l',2]\sqrt{\frac{3}{4\pi}}\begin{pmatrix}l & 2 & l'\\ 0 & 0 & 0\end{pmatrix} \tag{C5}$$

$$\langle S||S^{(2)}||S'\rangle = \delta_{S,S'}\delta_{S,1}\sqrt{\frac{5}{4}},$$

so

$$\begin{aligned}&\langle SM_S\,l\,m|H_{\rm dip}|S'M'_S\,l'm'\rangle\\ &= \delta_{S,S'}\delta_{S,1}\frac{3\alpha^2}{2R^3}\sum_q(-1)^{q-M_S-m}\begin{pmatrix}1 & 2 & 1\\ -M_S & -q & M'_S\end{pmatrix}\\ &\quad\times\begin{pmatrix}l & 2 & l'\\ -m & q & m'\end{pmatrix}\begin{pmatrix}l & 2 & l'\\ 0 & 0 & 0\end{pmatrix}.\end{aligned} \tag{C6}$$

The $3j$ symbol selection rules require $l=l'; l=l'\pm 2$ and so use of this representation leads to an infinite coupled set of partial waves [29]. We can re-express the scattering amplitude

$$\begin{aligned}F(\mathbf{R}) &= \sum_{Sl}\sum_{JM}\frac{G^{JM}_{Sl}(R)}{R}|JMSl\rangle\\ |JMSl\rangle &= \sum_m\sum_{M_S}Y_{lm}(\theta\phi)\sqrt{2J+1}\begin{pmatrix}S & l & J\\ M_S & m & -M\end{pmatrix},\end{aligned} \tag{C7}$$

and the matrix coupling elements in the resulting coupled radial equations are given by $\langle J'M'l'S'|H_{\rm dip}|JMSl\rangle$. Since $H_{\rm dip}$ is a rank-0 tensor we have

$$\begin{aligned}&\langle J'M'l'S'|H_{\rm dip}|JMSl\rangle\\ &= \delta_{J,J'}\delta_{M,M'}(-1)^{J-M}\begin{pmatrix}J & 0 & J\\ M & 0 & -M\end{pmatrix}\\ &\quad\times v(R)\langle J'M'l'S'||Y^{(2)}\cdot S^{(2)}||JMSl\rangle.\end{aligned} \tag{C8}$$

Using standard Racah-algebra identities [31],

$$\begin{aligned}&\langle J'M'l'S'||Y^{(2)}\cdot S^{(2)}||JMSl\rangle\\ &= (-1)^{l+S'+J}[J]^{1/2}\begin{Bmatrix}l & S & J\\ S' & l' & 2\end{Bmatrix}\langle S||S^2||S'\rangle\langle l||Y^2||l'\rangle.\end{aligned} \tag{C9}$$

Combining Eq. (C9) with Eq. (C8) we obtain

$$\begin{aligned}&\langle J'M'l'S'|H_{\rm dip}|JMSl\rangle\\ &= \delta_{S,S'}\delta_{S,1}\delta_{J,J'}\delta_{M,M'}\frac{\alpha^2}{R^3}(-1)^{l+l'+J}\\ &\quad\times\sqrt{\frac{15}{2}}[l,l']^{1/2}\begin{Bmatrix}l & S & J\\ S' & l' & 2\end{Bmatrix}\begin{pmatrix}l & 2 & l'\\ 0 & 0 & 0\end{pmatrix}.\end{aligned} \tag{C10}$$

Using the channel quantum numbers given in Table I we find that Eq. (C10) reproduces the entries proportional to α^2 in Eq. (11).

APPENDIX D: BORN APPROXIMATION

In the Born approximation, the amplitude for a transition from internal state $|F_aM_aF_bM_b\rangle$ and relative atom motion wave number $\boldsymbol{k}_i$ into internal state $|F'_aM'_aF'_bM'_b\rangle$ and wave number $\boldsymbol{k}_f$ is given by the expression

$$\begin{aligned}&f^{F'_aM'_aF'_bM'_b}_{F_aM_aF_bM_b}(\boldsymbol{k}_i;\boldsymbol{k}_f)\\ &= -\frac{1}{4\pi}\frac{2\mu}{\hbar^2}\int d^3\boldsymbol{R}\exp[i\,\boldsymbol{R}(\boldsymbol{k}_i-\boldsymbol{k}_f)]\left\{\frac{-\alpha^2}{R^3}\sqrt{\frac{24\pi}{5}}\right.\\ &\quad\left.\times\sum_m(-1)^mY_{2m}(\theta\phi)\langle F_aM_aF_bM_b|S^{(2)}_m|F'_aM'_aF'_bM'_b\rangle\right\},\end{aligned} \tag{D1}$$

where we used Eq. (C3). Expressing the momentum transfer exponential as a partial wave expansion and performing the integrals we obtain

$$f^{F_a' M_a' F_b' M_b'}_{F_a M_a F_b M_b}(\boldsymbol{k}_i;\boldsymbol{k}_f) = (-1)^{q+1}\frac{2\mu\alpha^2}{\hbar^2}\sqrt{\frac{24\pi}{45}}\,Y^*_{2q}(\hat{\boldsymbol{u}}) \times \langle F_a M_a F_b M_b|S^{(2)}_q|F_a' M_a' F_b' M_b'\rangle,$$
$$q \equiv M_a + M_b - M_a' - M_b', \qquad \text{(D2)}$$
$$\hat{\boldsymbol{u}} \equiv \frac{\boldsymbol{k}_i - \boldsymbol{k}_f}{|\boldsymbol{k}_i - \boldsymbol{k}_f|}.$$

For heteronuclear systems the total spin-changing cross sections are

$$\sigma(F_a M_a F_b M_b \to F_a' M_a' F_b' M_b') = \frac{k_f}{k_i}\frac{1}{4\pi}\int d\hat{\Omega}_i \int d\hat{\Omega}_f \left| f^{F_a' M_a' F_b' M_b'}_{F_a M_a F_b M_b}(\boldsymbol{k}_i;\boldsymbol{k}_f)\right|^2 = \frac{k_f}{k_i}\left(\frac{2\alpha^2\mu}{\hbar^2}\right)^2\frac{8\pi}{15}\left|\langle F_a M_a F_b M_b|S^{(2)}_q|F_a' M_a' F_b' M_b'\rangle\right|^2, \qquad \text{(D3)}$$

where we used

$$\frac{1}{4\pi}\int d\hat{\Omega}_f \int d\hat{\Omega}_i\; Y^*_{2q}(\hat{\boldsymbol{u}})Y_{2q}(\hat{\boldsymbol{u}}) = 1. \qquad \text{(D4)}$$

The homonuclear H-H and T-T pairs must satisfy bosonic exchange symmetry requirements and therefore

$$\sigma(F_a M_a F_b M_b \to F_a' M_a' F_b' M_b') = \frac{k_f}{k_i}\frac{1}{2}\frac{1}{4\pi} \int d\hat{\Omega}_i \int d\hat{\Omega}_f \left| f^{F_a' M_a' F_b' M_b'}_{F_a M_a F_b M_b}(\boldsymbol{k}_i;\boldsymbol{k}_f) + f^{F_b' M_b' F_a' M_a'}_{F_a M_a F_b M_b}(\boldsymbol{k}_i;-\boldsymbol{k}_f)\right|^2, \qquad \text{(D5)}$$

where we included the additional factor $1/2$ to avoid double counting during integration over all final angles of the differential cross section. Evaluating expression (D5) we obtain

$$\sigma(F_a M_a F_b M_b \to F_a' M_a' F_b' M_b') = \frac{k_f}{k_i}\left(\frac{2\alpha^2\mu}{\hbar^2}\right)^2\frac{4\pi}{15}[|\mathcal{D}|^2 + |\mathcal{E}|^2 + 2h(\xi)\,\mathcal{D}\,\mathcal{E}], \qquad \text{(D6)}$$

where

$$\xi \equiv \frac{k_f}{k_i},$$

and

$$\mathcal{D} \equiv \langle F_a M_a F_b M_b|S^{(2)}_Q|F_a' M_a' F_b' M_b'\rangle,$$
$$\mathcal{E} \equiv \langle F_a M_a F_b M_b|S^{(2)}_Q|F_b' M_b' F_a' M_a'\rangle. \qquad \text{(D7)}$$

In deriving expression (D6) we used Eq. (D4) and

$$\frac{1}{4\pi}\int d\hat{\Omega}_f \int d\hat{\Omega}_i\; Y^*_{2q}(\hat{\boldsymbol{u}})Y_{2q}(\hat{\boldsymbol{v}}) = h(\xi)/4$$
$$\hat{\boldsymbol{v}} \equiv \frac{\boldsymbol{k}_i + \boldsymbol{k}_f}{|\boldsymbol{k}_i + \boldsymbol{k}_f|}$$
$$h(\xi) = \frac{3(\xi^2-1)^2\log\left[\frac{(\xi+1)^2}{(\xi-1)^2}\right]}{8\xi(\xi^2+1)} - \frac{1}{2}, \qquad \text{(D8)}$$

for $\xi > 1$.

[1] H. I. Ewen and E. M. Purcell, Nature (London) **168**, 356 (1951).
[2] S. R. Furlanetto, S. P. Oh, and F. H. Briggs, Phys. Rep. **433**, 181 (2006).
[3] A. Loeb and M. Zaldarriaga, Phys. Rev. Lett. **92**, 211301 (2004).
[4] J. P. Wittke and R. H. Dicke, Phys. Rev. **103**, 620 (1956).
[5] E. M. Purcell and G. B. Field, Astrophys. J. **124**, 542 (1956).
[6] A. Dalgarno, Proc. R. Soc. London A **262**, 132 (1961).
[7] B. Zygelman, Astrophys. J. **622**, 1356 (2005).
[8] C. M. Hirata and K. Sigurdson, Mon. Not. R. Astron. Soc. **375**, 1241 (2007).
[9] B. Zygelman, A. Dalgarno, M. J. Jamieson, and P. C. Stancil, Phys. Rev. A **67**, 042715 (2003).
[10] A. C. Allison and A. Dalgarno, Astrophys. J. **158**, 423 (1969).
[11] B. Shizgal, J. Phys. B **12**, 3611 (1979).
[12] M. Desaintfuscien and C. Audoin, Phys. Rev. A **13**, 2070 (1976).
[13] C. Baumgarten *et al.*, European Physical Journal D **48**, 343 (2008).
[14] H. T. C. Stoof, J. M. V. A. Koelman, and B. J. Verhaar, Phys. Rev. B **38**, 4688 (1988).
[15] L. W. Anderson, F. M. Pipkin, and J. C. Baird, Phys. Rev. **120**, 1279 (1960).
[16] E. Narevicius, A. Libson, C. G. Parthey, I. Chavez, J. Narevicius, U. Even, and M. G. Raizen, Phys. Rev. Lett. **100**, 093003 (2008).
[17] S. D. Hogan, A. W. Wiederkehr, H. Schmutz, and F. Merkt, Phys. Rev. Lett. **101**, 143001 (2008).
[18] S. Hensler, J. Werner, A. Griesmaier, P. O. Schmidt, A. Görlitz, T. Pfau, S. Giovanazzi, and K. Rzażewski, App. Phys. B **77**, 765 (2003).
[19] B. Zygelman and J. D. Weinstein, Phys. Rev. A **78**, 012705 (2008).
[20] R. V. Krems, J. Kłos, M. F. Rode, M. M. Szczęśniak, G. Chałasiński, and A. Dalgarno, Phys. Rev. Lett. **94**, 013202 (2005).
[21] H. A. Bethe and E. E. Salpeter, *Quantum Mechanics of One- and Two-Electron Atoms* (Academic Press, New York, 1957).
[22] B. Zygelman, A. Dalgarno, and R. D. Sharma, Phys. Rev. A **49**, 2587 (1994).
[23] B. Zygelman, in *Proceedings of the Dalgarno Celebratory Symposium: Contributions to Atomic, Molecular, and Optical Physics, Astrophysics, and Atmospheric Physics*, edited by J. F. Babb, K. Kirby, and H. Sadeghpour (World Scientific, Singapore, 2009).

[24] M. J. Jamieson and B. Zygelman, Phys. Rev. A **64**, 032703 (2001).
[25] M. J. Jamieson, A. Dalgarno, and L. Wolniewicz, Phys. Rev. A **61**, 042705 (2000).
[26] X. Chu, M. J. Jamieson, and A. Dalgarno, J. Phys. B **36**, L415 (2003).
[27] D. Blume, B. D. Esry, C. H. Greene, N. N. Klausen, and G. J. Hanna, Phys. Rev. Lett. **89**, 163402 (2002).
[28] M. A. Nielsen and I. L. Chuang, *Quantum Computation and Quantum Information* (Cambridge University Press, New York, 2000).
[29] B. Zygelman, e-print arXiv:physics/0209052 (2002).
[30] R. V. Krems, G. C. Groenenboom, and A. Dalgarno, J. Phys. Chem. A **108**, 8941 (2004).
[31] A. de Shalit and I. Talmi, *Nuclear Shell Theory* (Academic Press, New York, 1963).